Biosensors and Bioelectronics 26 (2011) 3768–3773

Contents lists available at ScienceDirect

Biosensors and Bioelectronics

journal homepage: www.elsevier.com/locate/bios

A highly sensitive and specific biosensor for ligation- and PCR-free detection of MicroRNAs

Zhiqiang Gao[a,*], Yanfen Peng[b]

[a] Department of Chemistry, National University of Singapore, Singapore 117543, Singapore
[b] Institute of Bioengineering and Nanotechnology, 31 Biopolis Way, Singapore 138669, Singapore

ARTICLE INFO

Article history:
Received 7 December 2010
Received in revised form 11 February 2011
Accepted 18 February 2011
Available online 24 February 2011

Keywords:
MicroRNA
Amperometry
Glucose oxidase
Osmium
Exonuclease

ABSTRACT

A highly sensitive microRNA (miRNA) biosensor for both ligation- and PCR-free detection of miRNAs is described in this work. The biosensor was made of a monolayer of long oligonucleotide capture probes (CPs) comprising of miRNA capturing segments at the top (3′ termini) and detection probe capturing segments at the bottom (5′ termini). Following hybridization with a target miRNA, a cocktail of Surveyor® and exonuclease I in pH 7.4 phosphate buffered saline was applied to the biosensor. Unhybridized CP strands and mismatched miRNA/CP duplexes were digested while complementarily hybridized ones remained intact. Thereafter, electrochemically activated glucose oxidase-tagged peptide nucleic acid detection probes (GOx–DP) were hybridized to the bottom segments of the CPs on the biosensor. The number of GOx molecules found at the biosensor surface coincides with the number of miRNA strands hybridized and therefore correlates directly to the concentration of the target miRNA. A detection limit of 10 fM and a linear current–concentration relationship up to 10 pM were attained under optimized conditions. The biosensor effectively eliminated the needs for chemical/biological ligation and PCR. It was showed that there is little cross-hybridization among closely related miRNA family members even at single-base-mismatched levels. Successful attempts were made in applying the biosensor to the detection of miRNAs in total RNA extracted from cell lines.

1. Introduction

MicroRNAs (miRNAs) are highly conserved small RNA molecules (~22 nucleotides) encoded in the genomes of plants and animals. These small RNAs negatively regulate the expression of genes by binding to the 3′-untranslated regions of their target messenger RNAs (mRNAs) that either leads to mRNA degradation or translational repression (Bartel, 2004; Engels and Hutvagner, 2006). Up to date, 1048 miRNAs have been identified in the human genome (miRBase sequence database, 2010). It has been shown that each miRNA has the potential to regulate many target genes in humans, modulating the levels of thousands of mRNAs, implying that ≥50% of all protein encoding genes in humans are regulated by miRNAs (Lewis et al., 2005). Recent studies show that miRNAs also play important roles in a wide range of physiologic and pathologic processes (Stefani and Slack, 2008). Deregulations of miRNAs have been found in many diseased specimens and tumors in particular, making them strong candidate oncogenes and tumor suppressors (Calin and Croce, 2006; Esquela-Kerscher and Slack, 2006; Zhang et al., 2007; Croce and Calin, 2005). In future they even can be considered as excellent tools in molecular therapy approaches as well as in molecular diagnostics at the gene expression level.

Tremendous progress made in miRNA research in the past five years has opened the door to new perspectives in diagnostics and to a new promising therapeutic field. It also fueled the need to develop an accurate and inexpensive platform for miRNA expression profiling. Conventional technologies, such as Northern blotting and cloning traditionally used to analyze mRNAs, were initially adapted to study miRNAs. Both techniques have been informative to ascertain how miRNAs are spatially and temporally expressed and the former remains the gold standard of miRNA validation and quantification (Bartel, 2004; Valoczi et al., 2004). Nonetheless, tedious procedures, extremely time consuming, and the lack of sensitivity of the two techniques have prompted researchers to look for faster and more sensitive techniques, such as microarray and polymerase chain reaction (PCR)-based techniques. With a relatively large number of miRNAs to be studied, microarrays appear to be an ideal platform for high-throughput, multiplexed miRNA expression analysis. The small size and high sequence homology of miRNAs present major challenges to sample labeling and microarray probe design. Thus, miRNA microarrays must first engage an

* Corresponding author. Tel.: +65 6824 7113; fax: +65 6478 9085.
E-mail address: zqgao@ibn.a-star.edu.sg (Z. Gao).

0956-5663/$ – see front matter © 2011 Elsevier B.V. All rights reserved.
doi:10.1016/j.bios.2011.02.029

effective miRNA labeling procedure. Attempts to label miRNAs were mostly based on direct biochemical and chemical ligation and ligation (miRNA extension)–PCR amplification. Unfortunately, poor reliability and differential ligation efficiencies may compromise the quality of the data of ligation–PCR-based microarray (Valoczi et al., 2004).

In terms of sensitivity, quantitative real-time PCR (qRT-PCR) has become the method of choice for measuring expression levels of both coding and non-coding RNAs. However, as compared to mRNAs, several unique attributes of miRNAs, such as their relatively uniform and small size, the lack of poly (A) tails, tendency to cross hybridize to their target mRNAs with imperfect sequence homology, significant sequence homology among family members, and the similar sizes of mature miRNAs and standard PCR primers limit the direct application of conventional RT-PCR protocols to miRNA detection (Mitchell et al., 2008; Liu et al., 2004). With even shorter primers, there is little room to fine tune hybridization conditions and therefore dwindling the stringency of hybridization and the power of PCR amplification. The small size of miRNAs also makes selective hybridization difficulty. To work with mature miRNAs, they must first be lengthened either by primer extension through ligation (Calin et al., 2004) or by stem-looped primers (Raymond et al., 2005), generating extended sequences suitable for subsequent PCR amplifications. For example, in the stem-loop approach, a stem-looped primer was hybridized with its target miRNA and then reverse transcription was employed. A PCR primer pair was designed according to the miRNA sequence itself and the unfolded stem-loop primer and then RT-PCR was performed with a TaqMan probe. The base stacking of the stem enhances the thermal stability of the primer/RNA duplex, which improves on the RT efficiency of the relatively short RT primers and the double-stranded structure of the stem-loop primer prevents its nonspecific binding to other RNA strands, resulting in significant improvements in both sensitivity and selectivity (Chen et al., 2005). Based on the above two strategies, several qRT-PCR approaches for the simultaneous amplification and quantification of miRNAs have been developed recently. They combined the exceptional amplification power of PCR with quantitative detection of the amplified products in real time during each reaction cycle. In order to differentiate experimentally induced variations from true biological changes, numerous variables need to be carefully controlled. And the use of multiple references is generally accepted as the standard practice for qRT-PCR data normalization. A major constraint is, however, their limited multiplexing capacity. Running too many replicates as single reactions for a panel of miRNAs is not cost-effective and not feasible for small or rare samples. In addition, all PCR-based techniques only work with isolated and highly purified total RNA samples.

Because of the emerging diagnostic and prognostic values of miRNAs, the methods for their expression profiling should be highly sensitive, specific, and only analyze mature miRNAs. It is, therefore, imperative to improve the technologies mentioned above and to develop novel approaches with high sensitivity for miRNA expression profiling. In this report, we present a miRNA biosensor together with a novel detection protocol that meets the sensitivity requirement for direct miRNA expression profiling, enabling a more simplified detection with minimal background and with significantly enhanced specificity and sensitivity. This biosensor neither requires PCR amplification, nor the use of fluorescent ligation. MicroRNA expression profiling can therefore be performed in as little as 10 ng of total RNA, providing a much-needed platform for miRNA expression analysis. It is important to point out that this technology is not restricted to the detection of miRNAs. Rather it is an attractive candidate for the development of highly sensitive detection technologies for nucleic acids.

2. Experimental

2.1. Chemicals and materials

Thiolated oligonucleotide capture probes (CPs) comprising both miRNA and detection probe capturing segments used in this work were custom-made by Sigma–Aldrich (St. Louis, MO) and used as received. Biotinylated peptide nucleic acid detection probes (DPs) were obtained from Eurogentec (Herstal, Belgium). Other oligonucleotides were from 1st Base Pte Ltd. (Singapore). All other reagents were purchased from Sigma–Aldrich and used without further purification. Glucose oxidase avidin conjugate (GOx–A, where avidin provides anchoring sites for the PNA DPs) was purchased from Vector Laboratories (San Diego, CA). 1-Ethyl-3-(3-(dimethylamino) propyl)carbodimide hydrochloride (EDC), N-hydroxysulfosuccinimide (NHS) and dialysis kits (MWCO 10,000) were purchased from Pierce (Rockford, IL). Redox mediator $Os(bpy)_2(API)Cl$ was synthesized from K_2OsCl_6 followed a published procedure (Gao et al., 2002). Phosphate-buffered saline (PBS, 10 mM phosphate buffer + 139 mM NaCl + 2.7 mM KCl) was used in CP immobilization and exonuclease digestion. A pH 8.5 10 mM Tris–HCl– 1.0 mM EDTA–0.10 M NaCl–50 mM $MgCl_2$ (TEM) buffer solution was used as hybridization and washing buffer. Total RNA was extracted using TRIzol reagent (Invitrogen, Carlsbad, CA) according to the manufacturer's recommended protocol. To minimize the effect of RNases on the stability of miRNAs, diethyl pyrocarbonate treated deionized (DI) water was used for all sample and buffer preparations. And surfaces were decontaminated with RNaseZap (Ambion, TX). Gold electrodes were cleaned in hot Nanostrip® (Nanostrip®, Cyantek Corporation 2008) for 10 min, thoroughly rinsed with water, and dried in a stream of nitrogen immediately before CP immobilization.

2.2. Electrochemically activated GOx–DP synthesis

GOx was covalently modified with the redox mediator $Os(bpy)_2(API)Cl$ by amide bond formation between its carboxyls and the aliphatic primary amino group of $Os(bpy)_2(API)Cl$ with EDC/NHS as the coupling agents. Large excess mediator was used to avoid GOx–A self-crosslinking. Briefly, 10 mM EDC and 0.40 mM NHS were added to 1.0 ml PBS containing 1.0 mM $Os(bpy)_2(API)Cl$ and 10 μM GOx–A, respectively. The mixture was stirred for 12 h at 4 °C. The reaction mixture was purified by dialysis against PBS at 4 °C. The electrochemically activated GOx–A was attached to the PNA DP via biotin–avidin interaction at a GOx–A/DP ratio of 1:2. Free biotinylated DP was removed through a spin-column having a cut-off mass of 20 kD. The $Os(bpy)_2(API)Cl$ content in the activated GOx was determined by ICP mass spectrometry (ICP-MS, PerkinElmer, Wellesley, MA).

2.3. Hybridization and detection

MicroRNA detection was carried out as illustrated in Scheme 1. (a) The biosensor made of a monolayer of long oligonucleotide CPs comprising miRNA and GOx–DP capturing segments, was first hybridized for 60 min at room temperature with aliquots of 2.0 μl of miRNA sample solution in TEM buffer where the top miRNA capturing segments of the CPs collect their corresponding target miRNAs and possibly together with other imperfectly matched interfering miRNAs. (b) The hybridized biosensor was then incubated in the cocktail of Surveyor® and nuclease I in pH 7.4 PBS for 30 min at 37 °C. (c) At this stage, imperfectly hybridized miRNA–CP duplexes and free CP strands on the biosensor were digested by Surveyor® (Qiu et al., 2004) and nuclease I (Shimada et al., 2010), respectively. (d) After a post-incubation clean-up, only the perfectly hybridized ones remained on the biosensor. (e) A solution

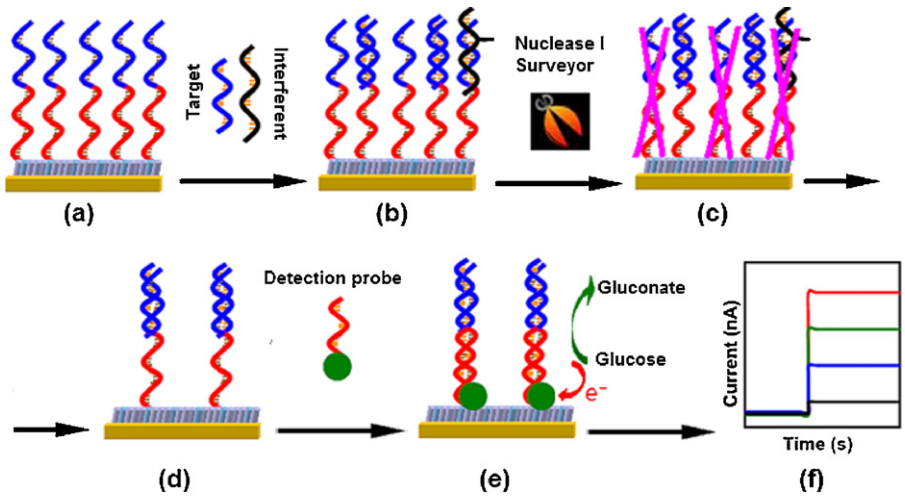

Scheme 1. Schematic illustration of the working principle of the miRNA biosensor.

containing the GOx–DPs is introduced onto the biosensor. Without the need for further discrimination, the GOx–DPs were hybridized with the bottom segments of all remaining strands, bringing GOx onto the biosensor. (f) The presence of GOx at the biosensor surface created an efficient bioelectrocatalytic system for the oxidation of glucose and provided much needed sensitivity for the detection of miRNA. Since each GOx molecule, conjugated to DP, signaled a perfectly hybridized miRNA, the surface coverage of GOx and hence the catalytic power manifested the concentration of the target miRNA in the sample. Glucose electrooxidation current was measured amperometrically in PBS containing 60 mM glucose at room temperature with the biosensor poised at 0.30 V (vs. Ag/AgCl).

3. Results and discussion

3.1. Electrochemical activation of GOx–DP

Fig. 1(a) depicts UV–Vis absorption spectra of the $Os(bpy)_2(API)Cl$ activated and native GOx–A. The spectrum of the activated GOx–A (trace 3) was roughly a composite of the absorption spectra (trace 4) of both native GOx–A (trace 2) and $Os(bpy)_2(API)Cl$ (trace 1). $Os(bpy)_2(API)Cl$ in the activated GOx–A was determined by ICP-MS. The ratio of $Os(bpy)_2(API)Cl$ to GOx–A was found to be ~45/1. To prove that $Os(bpy)_2(API)Cl$ is indeed covalently tethered to GOx–A, as opposed to simple electrostatic association with GOx–A, control experiments were performed in the absence of the EDC/NHS coupling reagents. The UV–Vis spectrum of thus treated GOx–A was practically identical to that of native GOx–A and no detectable redox activities were observed, implying that $Os(bpy)_2(API)Cl$ is unlikely electrostatically bonded to GOx–A.

To assess whether the activated GOx–A retains its biological integrities, after purification 5 μl of 1.0 mg/ml of the activated GOx–A was applied to a biotin monolayer-coated gold electrode. After 10 min incubation at room temperature, the GOx–A solution was rinsed off and the electrode was thoroughly cleaned in PBS. A typical cyclic voltammogram of the electrode in PBS is shown in trace 1 in Fig. 1(b). Unlike the featureless voltammogram of native GOx–A (trace 2), the activated GOx–A showed a pair of well-defined voltammetric peaks centered at 0.13 V, indicating that $Os(bpy)_2(API)Cl$ moieties bonded to GOx–A effectively facilitate the transfer of electrons from the redox centers of GOx to the electrode and GOx becomes redox active after modification. The voltammetric response can, in principle, be utilized for the detection of miRNAs. However, as inherent to voltammetry, a

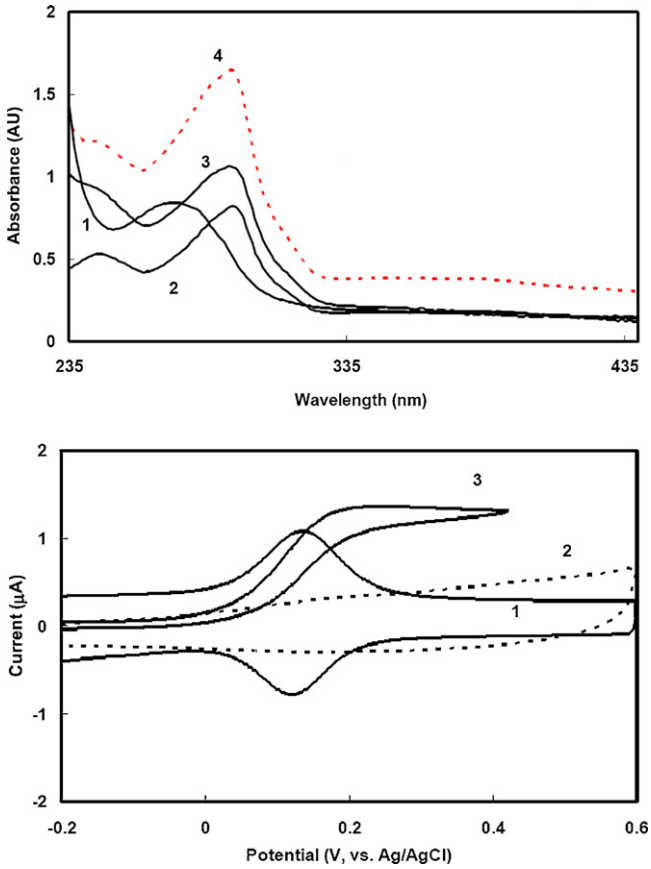

Fig. 1. Top (a) Normalized UV–Vis spectra of (1) $Os(bpy)_2(API)Cl$, (2) native GOx–A, (3) the activated GOx–A, and (4) composite of (1) and (2). Bottom (b) Cyclic voltammograms of (1) the activated GOx–A (100 mV/s), (2) native GOx–A (100 mV/s) in PBS, and (1) +60 mM glucose (25 mV/s).

considerable background current was obtained, making voltammetry unfavorable in developing ultrasensitive miRNA biosensors. In contrast, the charging current in amperometry diminishes quickly to sub-nanoampere levels after a potential bias is applied. With this much reduced background, high sensitivity may be anticipated.

Enzymatic oxidation of glucose was further carried out and monitored voltammetrically upon the addition of glucose to PBS. As glucose was added, obvious catalytic current was observed due to the presence of GOx–A at the electrode surface (Fig. 1(b) trace

3). The electrode responded rapidly achieving a steady-state at scan rates <25 mV/s, implying that GOx retains its catalytic activity toward the oxidation of glucose. The sigmoidal feature of the catalytic oxidation of glucose shows that the activated GOx is an excellent electrocatalyst for the electrooxidation of glucose with a very high catalytic rate constant (Murray, 1984; Gregg and Heller, 1991; Gao and Siow, 1996; Molina et al., 2009). The good redox activity and catalytic efficiency of the activated GOx suggest that it can be used as a bioelectrocatalytic tag/amplifier in the development of highly sensitive biosensors. To prove that the glucose oxidase was activated by the covalently bound redox mediator, not by direct electron-exchange with the substrate electrode, native GOx–A treated electrode was tested in the same solution. No detectable glucose oxidation current was observed in the potential range of 0.0–0.8 V, obviously due to the lack of the redox activator in the system. It implies that the reaction centers of GOx cannot exchange electrons directly with the gold electrode. Similar conclusion can be found in literature (Heller, 1990; Xie et al., 2004).

3.2. Feasibility of miRNA detection

Fig. 2 compares glucose oxidation currents in amperometry generated by the biosensor with a let-7b biosensor when hybridized to let-7 family miRNAs in the absence (control) and in the presence of different amounts of let-7b. Upon hybridization, let-7b was selectively captured and bound to the biosensor, where little if any of other members of the let-7 family was captured during hybridization. As expected, a minimal change barely distinguishable form the background (trace 1) was observed after hybridization to all other members of the let-7 family at a relative high concentration of 210 pM. As shown in traces 2–4 in Fig. 2, after hybridization with different amounts of let-7b, substantial increases in the oxidation current were observed in all cases and the current increased by as much as 20-fold in the presence of only 1.0 pM let-7b. It was found that extensive washing produces no noticeable changes, revealing that the GOx–DPs are robustly bound to the CPs, most probably through base-pairing to the CPs. The sizeable increase in current and its dependence on let-7b concentration clearly indicated that the formation of CP–GOx–DP duplexes is guided by the hybridized miRNA strands and the resulted GOx on the biosensor surface effectively catalyzes the oxidation of glucose. The extremely low current of the control implies that the imperfect hybridization-related signal of this biosensor array is negligible, which facilitates the detection of miRNA at ultralow concentrations. This may be attributed to the use of the exonuclease cocktail and the two-step hybridization.

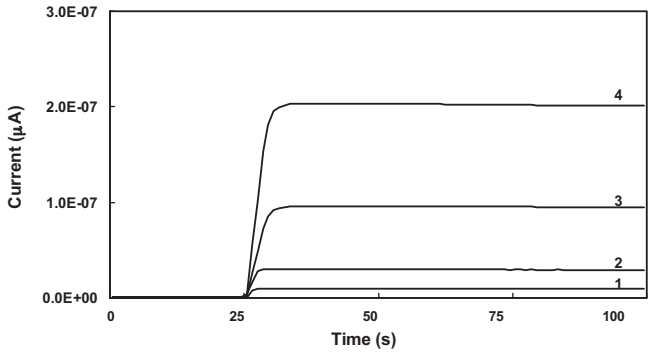

Fig. 2. Amperometric responses of (1) 0, (2) 0.1, (3) 0.5, and (4) 1.0 pM let-7b in the presence of 210 pM other let-7 miRNAs at equal molarities.

3.3. Optimization

The above experiments suggest that the GOx–DP can be used as an amplifier in constructing an ultrasensitive miRNA biosensor. The feature of bioelectrocatalysis that appears to be particularly promising is the extremely low potential at which glucose oxidation takes place. Electrochemical detection at a significantly lower operating potential minimizes potential interferences and reduces the background signal, yielding an improved signal/noise ratio and a low detection limit. To successfully utilize the activated GOx as the amplifier, the overall signal (current response) of the biosensor should be simply proportional to the number of GOx molecules present at the biosensor surface. This oversimplified current–GOx relationship can only be fulfilled under extremely stringent conditions where the current is solely controlled by the catalytic turnover of the activated GOx. In the case of the bioelectrocatalytic oxidation of glucose by the activated GOx, the oxidation current must be determined by one or a combination of the following processes: (i) mass-transport process of glucose in solution, (ii) catalytic turnover of the activated GOx, and (iii) electron-transfer at the GOx–electrode interface. Under extreme circumstances, when both the electron transfer and the mass-transport are much faster than the catalytic turnover, the oxidation current is then solely controlled by the catalytic turnover of the activated GOx, which in turn, by the total number of GOx tags at the biosensor surface, and thereby by the concentration of the analyzed miRNA in solution. This sole catalysis-controlled process can be achieved by "speeding up" both mass-transport and electron-transfer rates because little can be conveniently done in modulating the catalytic power of the activated GOx. The mass-transport rate is directly proportional to the concentration of glucose. High mass-transport rates are obtained when working with high concentrations of glucose. As shown in Fig. 3(a), the catalytic current was practically independent of glucose concentration at ≥50 mM, suggesting that the mass transport in solution now is

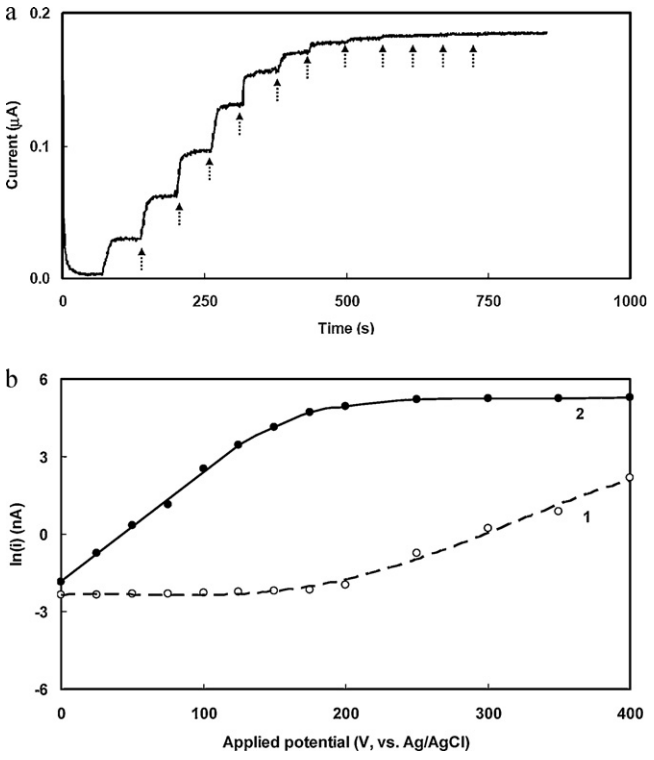

Fig. 3. (a) Effect of glucose concentration and (b) applied potential on the amperometric response of 1.0 pM let-7b. Arrows denote the additions of glucose in 5-mM increments.

fast enough that it is not the rate (current)-determining process. Meanwhile, a high electron-transfer rate is achievable by increasing the energy level gap between the electrons at the GOx and at the substrate gold electrode as the electron-transfer rate increases exponentially with increasing the energy level gap according to the Bulter–Volmer equation (Bard and Faulkner, 2001). As illustrated in trace 2 Fig. 3(b), the linear segment of the ln(i) vs. E plot indicated that the overall process is controlled by the electron-transfer at the GOx–electrode interface. The increase in oxidation current with a more positive potential is due to the increase in electron-transfer rate (charge collection efficiency), as the electrons generated during the oxidation of glucose will be more efficiently collected by the electrode (Bard and Faulkner, 2001). The level-off potential was found to be ~0.20 V. 100 mV above the level-off potential, all electrons generated during the oxidation are collected by the electrode. And the oxidation current now was practically independent of the applied potential as the applied potential increased further. The deviations from linearity at higher applied potentials come from limitations imposed by bioelectrocatalysis, as the electron-transfer rate is accelerated to such an extent that bioelectrocatalysis is becoming the rate-limiting step. The above experiments reveal that a sole catalytic turnover controlled oxidation of glucose exists under conditions of high glucose concentrations (≥50 mM) and high applied potentials (>0.30 V). However, as shown in trace 1 in Fig. 3(b), too high an applied potential substantially lifted the background current. 0.30 V and 60 mM glucose were therefore selected for subsequent experiments.

3.4. Analytical characteristics of the biosensor

The analytical performance of the biosensor was tested on three mature human miRNAs, namely hsa-miR-720 (miR-720, 17 nt), hsa-let-7b (let-7b, 22 nt), and hsa-miR-1248 (miR-1248, 27 nt), covering from the shortest (17 nt) to the longest (27 nt) miRNAs. The corresponding synthetic miRNAs were used as calibration standards. Six replicates were tested for each miRNA. The 60-min incubation period generated a dynamic range of 20 fM to 10 pM with a relative standard derivation of <15% at 1.0 pM (6 duplicates) (Fig. 4(a)). The detection limit, defined as a signal/noise ratio of 3.0, was found to be ~10 fM (20 zmol). Compared to previous miRNA biosensors, the sensitivity was greatly improved over two orders of magnitude (Gao and Yang, 2006; Qavi et al., 2010; Fan et al., 2007) through the combination of the direct and full-length hybridization, exonuclease digestion, and the activated GOx–DP application. In this biosensor the ratio of GOx to hybridized target miRNA strands is fixed at one. The amount of the CPs immobilized on the biosensor and hybridization efficiency dictate the amount of hybridized target miRNA and thereby the amount of GOx found at the biosensor. Since the first hybridization was carried at very low stringency to ensure maximal hybridization efficiencies for all target miRNAs, the effect of melting temperature is largely minimized. At the same molar concentration, the sensitivity should be roughly independent of the size of miRNAs. Indeed, as shown in Fig. 4(a), a practically constant sensitivity for all three miRNAs tested was obtained irrespective to their lengths, confirming that there is little effect by the vast difference in melting temperature (T_m), as large as 30 °C, and therefore the hybridization efficiency for all miRNAs are practically equal irrespective of their lengths.

The specificity of the biosensor was evaluated by analyzing let-7 family members with a biosensor only complementary to let-7b. Between let-7b and let-7c, and let7-b and let-7a, there are one- and two-nucleotide differences out of 22 nucleotides, meaning that the let-7b biosensor is one and two base-mismatched for let-7c and let-7a, respectively. As shown in Fig. 4(b), the currents dropped by as much as ~98% and 99% when let-7c and let-7a were tested at the let-7b biosensor, which translate into a single-base mismatch

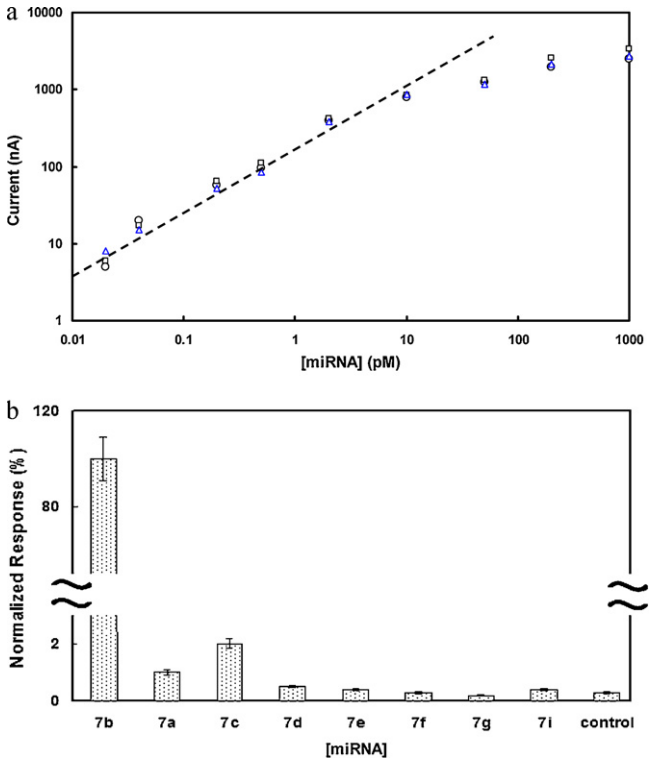

Fig. 4. (a) Calibration curves for (○) miR-720, (△) let-7b, and (□) miR-1248. (b) Normalized amperometric responses of a let-7b biosensor to other let-7 miRNAs at 1.0 pM.

selectivity of ~50/1 and two-base mismatch selectivity of ~99/1, respectively. Moreover, the current was indistinguishable from the background level when three or more base-mismatched miRNAs were tested, for example, let-7d, let-7e, let-7f, let-7g, let-7h, and let-7i tested at the let-7b biosensor. This mismatch discrimination is far better than most optical and electrochemical nucleic acid biosensors (Tansil et al., 2005; Qavi et al., 2010; Fan et al., 2007). We believe that the excellent mismatch discrimination is originated form the combination of the use of Surveyor® and exonuclease I, and the unique two-segmented CPs. Since the conditions for the first hybridization are set to level off T_m effect, it is expected that some imperfectly matched miRNAs are also captured by the CPs. However, they are subsequently eliminated (cleaved) by Surveyor® and the corresponding CPs are digested by exonuclease I during the incubation in the cocktail. Therefore, each quantified result represents the specific quantity of a single miRNA and not the combined quantity of the entire family.

3.5. Sample analysis

The biosensor was applied to the analysis of three let-7 miRNAs in total RNA extracted from various cells, to determine its ability in quantifying miRNAs in real samples. As listed in Table 1. These results are in good agreement with those obtained by qRT-PCR on the same sample and consistent with recently published data of miRNA expression profiles (Barad et al., 2004; Allawi et al., 2004; Nelson et al., 2004). With the greatly improved sensitivity, the biosensor also significantly reduced the amount of total RNA needed from micrograms to nanograms, corresponding to <100 cells (Nelson et al., 2004; Lim et al., 2003). Relative errors associated with the biosensor were generally less than 15% in the concentration range of 100 fM to 10 pM. This is advantageous because the expressions of many of the most interesting miRNAs often differ slightly under different conditions.

Table 1
Analysis of miRNA in total RNA extracted from cell lines.

	let-7a (10^6 copy/μg RNA)	Let-7b (10^6 copy/μg RNA)	Let-7c (10^6copy/μg RNA)
HeLa cells	7.6 ± 1.2 (8.5 ± 1.0)[a]	16 ± 2.3 (19 ± 2.8)	6.9 ± 0.81 (7.9 ± 0.79)
Lung cancer cells	2.8 ± 0.32 (2.3 ± 0.18)	2.1 ± 0.32 (2.5 ± 0.35)	2.5 ± 0.28 (2.2 ± 0.24)
Normal cells	3.7 ± 0.60 (4.5 ± 0.39)	8.6 ± 0.94 (9.4 ± 0.98)	7.3 ± 0.89 (6.8 ± 0.76)

[a] Data in brackets were obtained by qRT-PCR.

4. Conclusion

We have developed a simple, highly sensitive and specific biosensor for PCR-free and ligation-free miRNA expression profiling. Without the need for elaborated sample preparation, it can potentially meet the need for a rapid, sensitive, and specific tool for profiling of miRNAs in molecular diagnostics and in molecular biological research. The high signal-to-noise ratio, demonstrated excellent single base-mismatch selectivity, and the amplification-free and ligation-free approach enhance the suitability of this biosensor for adapting to a miniaturized analytical platform. The freedom from cloning, ligation, and amplification, and the abilities to form a low density biosensor array open a path to molecular diagnostics, particularly for early cancer diagnosis, point-of-care and field uses.

Acknowledgements

We greatly appreciate the financial support provided by the A*STAR-ANR Program. Y.F.P. thanks A*STAR Graduate Academy for her SINGA Scholarship.

References

Allawi, H.T., Dahlberg, J.E., Olson, S., Lund, E., Olson, M., Ma, W.P., Takova, T., Neri, B.P., Lyamichev, V.I., 2004. RNA 10, 1153–1161.
Barad, O., Meiri, E., Avniel, A., Aharonov, R., Barsilai, A., Bentwich, I., Einav, U., Gilad, S., Hurhan, P., Karov, Y., Lobenhofer, E.K., Sharon, E., Shiboleth, Y.M., Shtutman, M., Bentwich, Z., Einay, P., 2004. Genome Res. 14, 2486–2494.
Bard, A.J., Faulkner, L.R., 2001. Electrochemical Methods. John Wiley & Sons, New York.
Bartel, D.P., 2004. Cell 116, 281–297.
Calin, G.A., Croce, C.M., 2006. Nat. Rev. Cancer 6, 857–866.
Calin, G.A., Liu, C.G., Sevignani, C., Ferracin, M., Felli, N., Dumitru, C.D., Shimizu, M., Cimmino, A., Zupo, S., Dono, M., 2004. Proc. Natl. Acad. Sci. U.S.A. 101, 11755–11760.
Chen, C., et al., 2005. Nucleic Acids Res. 33, e179.
Croce, C.M., Calin, G.A., 2005. Cell 122, 6–7.
Engels, B.M., Hutvagner, G., 2006. Oncogene 25, 6163–6169.
Esquela-Kerscher, A., Slack, F.J., 2006. Nat. Rev. Cancer 6, 259–269.
Fan, Y., Chen, X.T., Kong, J.M., Tong, C.H., Gao, Z.Q., 2007. Angew. Chem. Int. Ed. 46, 2051–2054.
Gao, Z.Q., Siow, K.S., 1996. Electroanalysis 8, 602–606.
Gao, Z.Q., Binyamin, G., Kim, H., Barton, S.C., Zhang, Y., Heller, A., 2002. Angew. Chem. Int. Ed. 41, 810–813.
Gao, Z.Q., Yang, Z.C., 2006. Anal. Chem 78, 1470–1477.
Gregg, B.A., Heller, A., 1991. J. Phys. Chem. 95, 5976–5980.
Heller, A., 1990. Acc. Chem. Res. 23, 128–134.
Lewis, B.P., Burge, C.B., Bartel, D.P., 2005. Cell 120, 15–20.
Lim, L.P., Lau, N.C., Weinstein, E.G., Abdelhakim, A., Yekta, S., Roades, M.W., Burge, C.B., Bartel, D.P., 2003. Gene Dev. 17, 991–1008.
Liu, C.G., Calin, G.A., Meloon, B., Gamliel, N., Sevignani, C., Ferracin, M., Dumitru, C.D., Shimizu, M., Zupo, S., Dono, M., 2004. Proc. Natl. Acad. Sci. U.S.A. 101, 9740–9744.
miRBase sequence database, 2010. http://www.mirbase.org, Release 15.0.
Mitchell, P.S., et al., 2008. Proc. Natl. Acad. Sci. U.S.A. 105, 10513–10518.
Molina, A., Soto, C.M., Gonzalez, J., 2009. Anal. Chem. 81, 6830–6836.
Murray, R.W., 1984. In: Bard, A.J. (Ed.), Nanostrip® Solution is a Mixture of H_2SO_4, H_2SO_5, H_2O_2, and Water, Available Commercially from Cyantek Corporation 2008, vol. 13. Marcel Dekker, New York, p. 191.
Nelson, P.T., Baldwin, D.A., Scearce, L.M., Oberholtzer, J.C., Tobias, J.W., Mourelatos, Z., 2004. Nat. Methods 1, 155–161.
Qavi, A.J., Kindt, J.T., Bailey, R.C., 2010. Anal. Bioanal. Chem. 398, 2535–2549.
Qiu, P., Shandilya, H., Alessio, J.M., O'Connor, K., Durocher, J., Gerard, G.F., 2004. BioTechniques 36, 702–707.
Raymond, C.K., Roberts, B.S., Garrett-Engele, P., Lim, L.P., Johnson, J.M., 2005. RNA 11, 1737–1744.
Shimada, A., Masui1, R., Nakagawa, N., Takahata, Y., Kim, K., Kuramitsu, S., Fukui, K., 2010. Nucleic Acids Res. 38, 5692–5705.
Stefani, G., Slack, F.J., 2008. Nat. Rev. Mol. Cell Biol. 9, 219–230.
Tansil, N.C., Xie, H., Xie, F., Gao, Z.Q., 2005. Anal. Chem. 77, 126–134.
Valoczi, A., Hornyik, C., Varga, N., Burgyan, J., Kauppinen, S., Havelda, Z., 2004. Nucleic Acids Res. 32, e175.
Xie, H., Zhang, C., Gao, Z.Q., 2004. Anal. Chem. 76, 1611–1617.
Zhang, B.H., Pan, X.P., Cobb, G.P., Anderson, T.A., 2007. Dev. Biol. 302, 1–12.